

# LOW-WIND-SPEED SMALL-SCALE WIND TURBINES FOR RURAL ELECTRIFICATION IN SRI LANKA

Mahinsasa Narayana

National Engineering Research and Development Centre of Sri Lanka,  
Ekala, Ja-Ela, Sri Lanka, Fax: ++94-11-5354597, E-mail: [narayana@nerdc.lk](mailto:narayana@nerdc.lk)

## 1. Introduction

The main objective of this study was to develop a low-wind-speed 100W capacity wind turbine generator (WTG) for rural electrification in Sri Lanka. Improve the performance of the rotor to extract more energy from low wind-speeds, in order to it is necessary to reduce the cut-in wind speed and design wind speed of WTG. Low starting torque of wind rotors has been identified as a main restriction against the reduction of cut-in wind speed of WTGs. This study intends to analyse the aerodynamics of wind rotors theoretically and thereby introduce appropriate changes to the geometrical parameters of the blades. Especially, the possibility of increasing the solidity of the rotor, without adversely affecting its aerodynamic efficiency was analysed. The blade elementary theory and the momentum theory were used to analyse the aerodynamic performance of rotors theoretically. In this project a wind rotor was developed for an existing 100W permanent magnet generator (PMG).

## 2. Aerodynamic Performance of Wind Rotors

The performance of the wind rotor is theoretically predicted by considering the wake-rotation of the wind-rotor by applying blade element theory and momentum theory, where the geometrical parameters ( $\beta$  - blade angles,  $l$  - chord lengths of each blade elements) of the existing blade are used. The characteristic performance of a wind-rotor is usually given by the variation of power coefficient ( $C_p$ ) with respect to the tip-speed ratio ( $\lambda_0$ ).

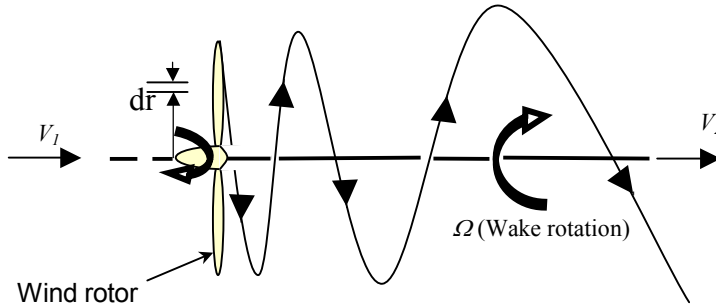


**Figure 1: Flow behind the rotor with wake-rotational effect**

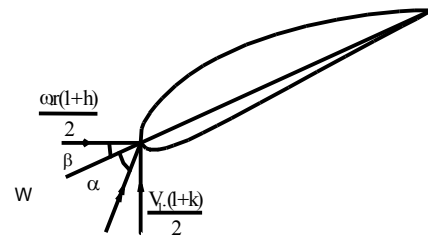


**Figure 2: Velocity diagram of a blade element**

Downstream of the rotor (Figure 1), the rotational speed of the wind flow is  $\Omega$ . Hence,  $\Omega = h\omega$ . Let,  $V_2 = kV_1$ . Where,  $V_1$  - wind speed,  $h$  - radial flow interference factor and  $k$  - axial flow interference factor.

Considering the blade element theory, axial thrust  $dF$  is given by:

$$dF = b.d.F_v = \frac{\frac{1}{2} \cdot \rho \cdot l \cdot W^2 \cdot b \cdot C_l \cdot \cos(\phi - \varepsilon) \cdot dr}{\cos \varepsilon} \quad (1)$$

Aerodynamic torque,  $dM$ , is given by:

$$dM = r.b.dF_u = \frac{1/2 \cdot \rho \cdot b \cdot l \cdot r \cdot W^2 \cdot C_l \cdot \sin(\phi - \varepsilon) \cdot dr}{\cos \varepsilon} \quad (2)$$

where,  $C_l$  - coefficient of lift,  $C_d$  - coefficient of drag,  $\tan \varepsilon = C_d/C_l$ ,  $\rho$  - air density,  $b$  - number of blades of wind rotor  $W$  - wind speed relative to the wind rotor,  $l$  - chord length of blade element, incidence angle  $(\phi) = \alpha + \beta$ ,

The above two values,  $dF$  and  $dM$ , can be determined by the general dynamics theory. Consider the axial momentum of the flow through the annulus:

Thrust = (rate of mass flow,  $m$ , through the element)  $\times$  (change in the axial velocity).

$$\text{Then, axial thrust, } dF = \rho \cdot \pi \cdot r \cdot dr \cdot V_1^2 \cdot (1 - k^2) \quad (3)$$

$$\text{Aerodynamic torque, } dM = \rho \cdot \pi \cdot r^3 \cdot dr \cdot \omega \cdot V_1 \cdot (1 + k) \cdot (h - 1) \quad (4)$$

Comparing the expressions for axial thrust and aerodynamic torque derived by blade elementary theory with that derived by momentum consideration given in equations [1].

$$\frac{1 - k}{1 + k} = \frac{C_l \cdot b \cdot l \cdot \cos(\phi - \varepsilon)}{8 \cdot \pi \cdot r \cdot \cos \varepsilon \cdot \sin^2 \phi} \quad (5)$$

$$\frac{h - 1}{1 + h} = \frac{C_l \cdot b \cdot l \cdot \sin(\phi - \varepsilon)}{4 \cdot \pi \cdot r \cdot \sin 2\phi \cdot \cos \varepsilon} \quad (6)$$

The wind rotor is divided in to 10 equal sections and the  $C_p$  value for each section was calculated by using the iterative procedure. The curve of coefficient of lift ( $C_l$ ) and of coefficient of drag ( $C_d$ ) verses the angle of attack ( $\alpha$ ) of the blade profile NACA 4415 was used for this calculation [2]. Then, coefficient of performance of the wind rotor segment at radius  $r$  ( $C_{pr}$ ) with respect to different tip speed ratios ( $\lambda_0$ ) was calculated.

$$C_{pr} = \frac{dP_u}{\rho \cdot \pi \cdot r \cdot dr \cdot V^3} = \lambda^2 \cdot (1 + k) \cdot (h - 1) \quad (7)$$

Then, coefficient of performance of the wind rotor ( $C_p$ ) is derived as follows.

$$C_p = \frac{2}{R^2} \cdot \int_r^R C_{pr} \cdot r \cdot dr \quad (8)$$

### 3. Design of a Wind Rotor Suitable for Low Wind Potential

Before discussing the design of a high solidity rotor it is important to study the starting torque of the wind rotor together with starting torque of the PMG. The initial torque of the PMG was measured at no load condition. The measured value is 0.34 Nm [3]. When the PMG is coupled with the 24V-battery bank, it operates under no load condition until it generates 24V. Due to cogging effect of PMGs, it needs an initial torque to rotate even at the no-load condition. After performing many iterative calculations it has been found that the required rotor radius to generate the required starting torque at a specific solidity is 2.1m. The selected blade profile is NACA4415, and the selected number of blades is 4. Chord lengths and other geometrical parameters of the wind rotor are given in Table 1. The optimum blade angle should be found for the selected chord length of each blade section, to obtain higher performance of the rotor. By applying the blade elementary theory and momentum theory, the following relations can be obtained.

$$\frac{1 - k}{1 + k} = \frac{C_l (b \cdot l / R) \cos(\phi - \varepsilon)}{8 \pi (r / R) \cos \varepsilon \sin^2 \phi} \quad \text{and} \quad \frac{h - 1}{1 + h} = \frac{C_l (b \cdot l / R) \sin(\phi - \varepsilon)}{4 \pi (r / R) \sin 2\phi \cos \varepsilon}$$

**Table 1: Selected solidity of wind rotor to obtain the required higher torque coefficient ( $C_m$ )**

Radius (mm)	Chord (mm)	Radius (mm)	Chord (mm)	Radius (mm)	Chord (mm)
420	400.0 (Fixed)	1050	336.3	1680	272.5
630	378.8	1260	315.0	1890	251.3
840	357.5	1470	293.8	2100	230.0 (Fixed)

At the optimum blade angle,  $C_l/C_d$  should be minimum and optimum angle of attack ( $\alpha$ ) of the profile is known. If number of Blade ( $b$ ), Chord length ( $l$ ),  $C_l$ ,  $\varepsilon$  ( $\tan \varepsilon = C_d/C_l$ ), and speed-ratio ( $\lambda$ ) are known at a certain section of the rotor,  $k$  and  $h$  values of that particular section could be found for each angle  $\phi$ . At the optimum blade angle ( $\alpha_{opt} = 5^\circ$ ) of the NACA4415 profile,  $C_l = 0.95$ ,  $C_d = 0.008$ , and  $\varepsilon = 8.42 \times 10^{-3}$  rad. Considering a element of rotor blade (Figure 2), the following expression can be derived:

$$\cot \phi = \lambda \frac{1+h}{1+k} \quad (9)$$

$$\cot \phi - \lambda \frac{1+h}{1+k} \text{ Vs angle } \phi,$$

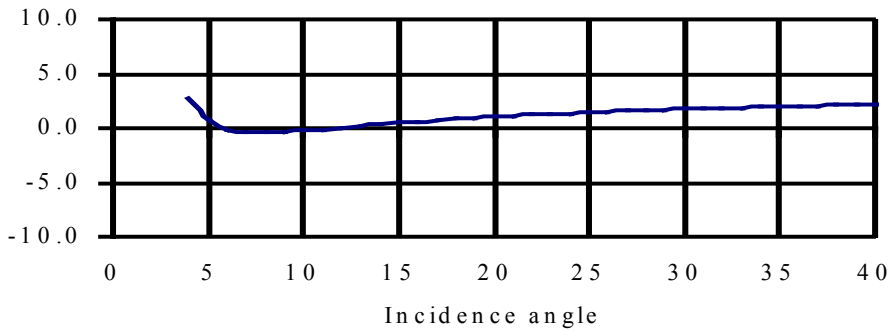


**Figure 3: Optimum incidence ( $\phi$ ) angle at the section  $r=0.9R=1980$  mm**

$$\cot \phi - \lambda \frac{1+h}{1+k} \text{ Vs angle } \phi,$$

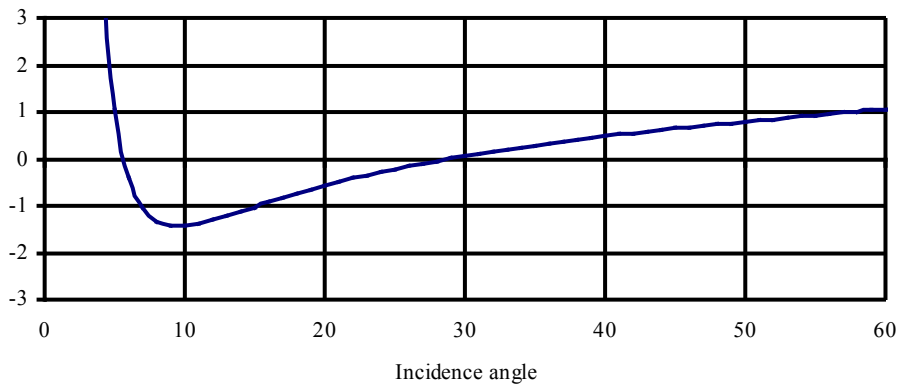


**Figure 4: Optimum incidence ( $\phi$ ) angle at the section  $r=0.4R=880$  mm**

Since  $h$  and  $k$  are functions of  $\phi$ , the above equation can be used to find the incidence angle ( $\phi$ ). However, even typical iterative methods do not give a convergent solution. Therefore a graphical method is used to find the solution. Here the graph of

$Y = \cot \phi - \lambda \frac{1+h}{1+k}$  is plotted and the intercept of the graph is located. To get a uniform twist of the blade, blade angles should be linearized, by using the blade angle at the section of 0.4R and 0.9R. Then, optimum incidence angles ( $\phi_{opt}$ ) are evaluated only at these sections. Solutions can be obtained by using Figure 3 and Figure 4. It has been noted that as the solidity of the rotor is increased the tip speed ratio should be decreased, to obtain a solution for  $\phi$  at the optimum. (Otherwise there is no solution to Equation (9)). In this design, solidity of the rotor is selected, while the blade-angle has been optimized. Suitable tip-speed ratio ( $\lambda_0$ ) of this optimization is 3.5. Note that, conventional wind rotors are designed for obtaining high efficiency so that both solidity and blade angles are optimized. In the present design the rotor has a higher solidity, than that corresponding to optimum solidity for  $\lambda_0=3.5$ . Optimum incidence angles, blade angles and chord lengths at the section  $r=0.4R$  and  $r=0.9R$  of the designed wind rotor are presented in Table 2.

**Table 2: Optimum incidence angles ( $\phi_{opt}$ ), blade angles and chord lengths at the section  $r=0.4R$  and  $r=0.9R$  of the designed wind rotor**

Radius (mm)	$\lambda, (\lambda_0=3.5)$	Chord length (mm)	Angle $\phi$ (Deg)	Angle $\beta$ (Deg)
0.9R=1890	3.15	257.5	11.6	6.6
0.4R=840	1.4	351.3	27.2	22.2

**Table 3: Geometrical parameters of high solidity wind rotor**

R (mm)	Blade angle $\beta$ (mm)	Chord, l (mm)	r (mm)	Blade angle $\beta$ (mm)	Chord, l (mm)	r (mm)	Blade angle $\beta$ (mm)	Chord, l (mm)
420	28.4	400.0	1050	19.1	336.3	1680	9.7	272.5
630	25.3	378.8	1260	16.0	315.0	1890	6.6	251.3
840	22.2	357.5	1470	12.8	293.8	2100	3.5	230.0

#### 4. Performance of the High Solidity Wind Rotor

The performance of the high solidity wind rotor is calculated theoretically by using the blade elementary theory and the momentum theory. Wind rotor is divided into 10 sections and the  $C_{pr}$  values are calculated for each section by using the searching procedure. Then  $C_p$  and  $C_m$  vs  $\lambda_0$  can be plotted for the rotor. The results are presented in Figure 6.

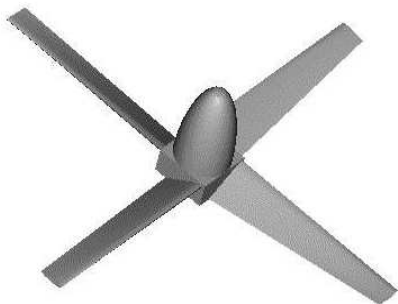


**Figure 5: High-solidity 4-bladed wind rotor**

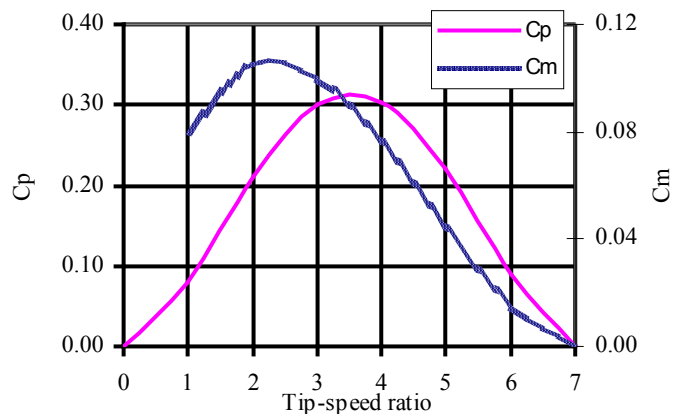


**Figure 6: Power coefficient curve of 4-bladed high solidity**

## 5. System Performance of the Developed Low-wind-speed Wind Turbine

The combined characteristics of the WTG can be predicted based on the individual characteristics of the rotor and the PMG. These characteristics are presented together in Figure 6, which shows the variation of power generated by the rotor at different wind speeds, and power output as a function of rotational speed. Note that the power input and output characteristics of PMG correspond to 24V battery load. The speed increase ratio between the rotor and the generator for optimum performance should be approximately 1:5. The performance characteristics of WTG with the wind speed predicted through Figure 6 are presented in Figure 7. This indicates that cut-in wind speed of WTG is 2.5m/s and the rated wind speed is 5m/s.

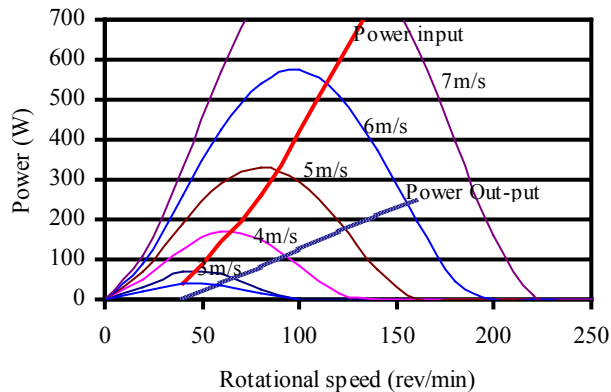


**Figure 6: Combine performance of 4 bladed rotor and PMG (With 1:5 Gear Box)**

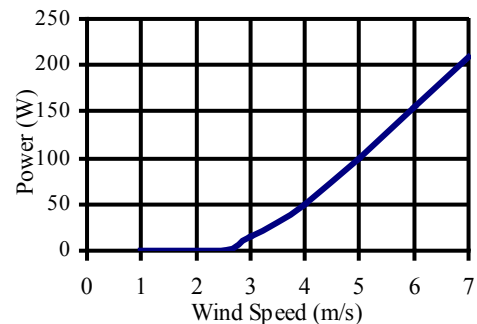


**Figure 7: Performance of high-solidity 4-bladed WTG**

## 6. Discussion

This study has been carried out to design a new wind rotor, which is suitable for low wind potential areas in Sri Lanka. A WTG for low wind-potential should be designed for low rated and cut-in wind speeds. When the rated wind speed is reduced, the diameter of the wind rotor should be increased in order to extract more energy from low wind-speeds. Low initial-torque of wind rotors is a main restriction against the reduction of the cut-in wind speed of WTG at low wind-speeds. Hence, solidity of the rotor should be increased to improve the starting torque, without affecting adversely its aerodynamic efficiency. In addition, in designing of a WTG, the wind rotor and the generator should properly match for its optimum operation.

## 7. References

- [1] Gourieres, D. Le. *Wind Power Plants Theory and Design*. Oxford: Pergamon press, 1982, pp76-120.
- [2] Abbott. Ira. H and Von Doenhoff. Albert. E. *Theory of Wing Section*, 1958, pp412 and pp490-491.
- [3] Narayana M, *Improved wind rotor design for a small-scale horizontal axis wind turbine suitable for local wind potential*. M.Phil. Thesis, University of Moratuwa, Sri Lanka, 2002, pp60